Available online at www.sciencedirect.com
ScienceDirect
Remote Sensing of Environment 107 (2007) 471–483
Remote Sensing of Environment
www.elsevier.com/locate/rse

Modelling and mapping potential hooded warbler (*Wilsonia citrina*) habitat using remotely sensed imagery

Jon Pasher, Doug King *, Kathryn Lindsay

Geomatics and Landscape Ecology Laboratory, Department of Geography and Environmental Studies, Carleton University, 1125 Colonel By Drive, Ottawa, Ontario, Canada K1S 5B6

Received 24 January 2006; received in revised form 25 September 2006; accepted 30 September 2006

Abstract

Modelling and mapping of hooded warbler (*Wilsonia citrina*) nesting habitat in forests of southern Ontario were conducted using Ikonos and Landsat data. The study began with an analysis of skyward hemispherical photography to determine canopy characteristics associated with nest sites. It showed that nest sites had significantly less overhead canopy cover and larger maximum gap size than in non-nest areas. These findings led to the hypothesis that brightness variability in high to moderate resolution remotely sensed imagery may be greater at nest sites than in non-nest areas due to larger shadows and greater shadow variability related to these gap characteristics. This was confirmed when, in addition to some spectral band brightness variables, several image texture and spectrally unmixed fraction (shadow, bare soil) variables were found to be significantly different for nest and non-nest sites in Ikonos and Landsat imagery. These significantly different variables were used in maximum likelihood classification (MLC) and logistic regression (LR) to produce maps of potential nesting habitat. Mapping was conducted with Ikonos and Landsat in a local area where most known nest sites occur, and regionally using Landsat data for almost all of the hooded warbler range in southern Ontario. For the local area mapping using Ikonos data, *a posteriori* probabilities for both the MLC and LR methods showed that about 62% of the nest sites set aside for validation had been classified with high probability ($p > 0.70$) in the nest class. MLC mapping accuracy was 70% for the validation nest sites and 87% of validation nest sites were within 10 m of classified nesting habitat, a distance approximately equivalent to expected positional error in the data. LR accuracy was slightly lower. Nest site MLC mapping accuracy in the local area using Landsat data was 87% but the map was much coarser due to the larger pixel size. Regional mapping with Landsat imagery produced lower classification accuracy due to high errors of commission for the habitat class. This resulted from a poor spatial distribution and low number of observations of nest sites throughout the region compared to the local area, while the non-nest site data distribution was too narrow, having been defined and assessed (using standard accepted methods) as areas with no ground shrubs. If either of these problems can be ameliorated, regional mapping accuracy may improve.

Keywords: Habitat mapping; Avian habitat; Hooded warbler; Hemispherical photography; Forest cover; Image texture; Spectral unmixing

1. Introduction

The protection of species at risk and the conservation of natural habitats are increasingly of concern due to human population growth and expansion. In Canada, habitat loss and fragmentation are due primarily to urbanization, the construction of roads, conversion of forests to agriculture, and resource extraction activities such as forestry and mining (Environment Canada, 2003). Hooded warblers (*Wilsonia citrina*) are currently listed as 'threatened' in Canada, with only 280 breeding pairs found in 2003 (SARA, 2005). This is higher than in 1992 when the number in Canada was estimated to be between 80 and 176 (Whittam & McCracken, 1999; Whittam et al., 2002), but the increase may reflect the more intensive surveys of recent years (Allair et al., 2002). These small neotropical migrants spend winters in areas of Mexico, Central America, and the Caribbean, and breed throughout the eastern United States and the Carolinian Forest of southwestern Ontario (Bisson & Stutchbury, 2000; Whittam et al., 2002). This paper

* Corresponding author. Tel.: +1 613 520 2600x8439; fax: +1 613 520 4301.
E-mail address: doug_king@carleton.ca (D. King).

0034-4257/$ - see front matter © 2006 Elsevier Inc. All rights reserved.
doi:10.1016/j.rse.2006.09.022

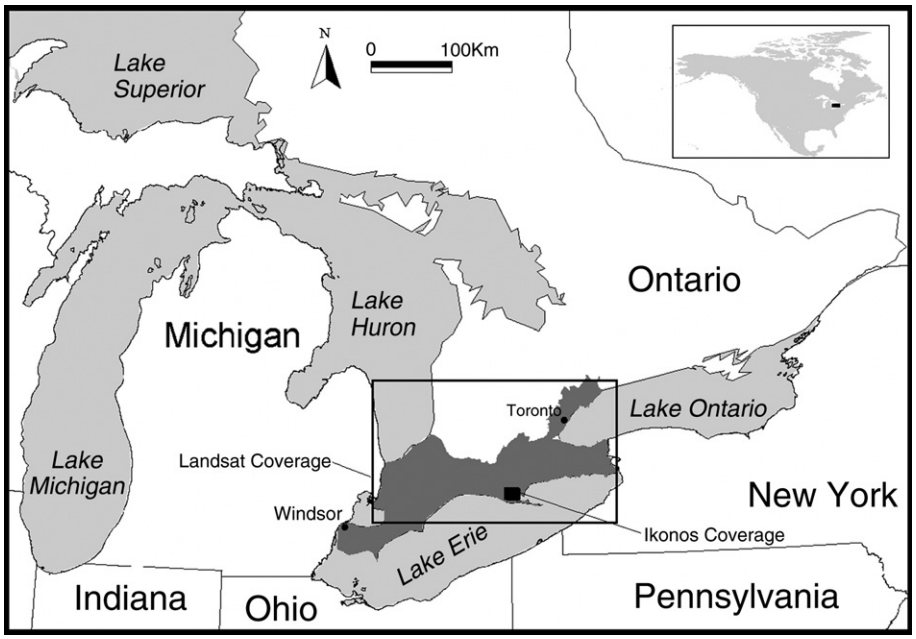

Fig. 1. The Carolinian Forest (dark shaded area) in southern Ontario. The Ikonos and Landsat data coverages are shown, indicating the local and regional study areas, respectively. Inset shows the study region (black rectangle) within North America.

presents research on modelling and mapping of hooded warbler habitat using remotely sensed imagery. Remote sensing can contribute to conservation programs by providing a means for mapping potential habitat if habitat characteristics for a given species can be associated with image spectral and spatial information.

There has been a significant amount of previous work examining nest site characteristics of the hooded warbler (Allair et al., 2002; Badzinski, 2003; Bisson & Stutchbury, 2000; Whittam & McCracken, 1999). It is usually found in areas of mixed hardwood forests that are moist with abundant ground vegetation. Nests are typically built within 1 m of the ground and supported by vines, stems or branches of species such as raspberry (*Rubus* spp.). Nest site locations have been found to be associated with overhead canopy gaps, (Allair et al., 2002; Bisson & Stutchbury, 2000; Whittam & McCracken, 1999), most likely as a result of the increased ground vegetation where light penetrates through the canopy (Rankin & Tramer, 2002).

James and McCulloch (2002) suggested that modelling habitat in order to produce maps describing the "presence, abundance, or absence" of species across larger geographic areas is of great importance for managing species at risk. There are many methods for mapping suitable habitat and species distributions, with a few of the more common ones involving supervised and unsupervised classification of satellite imagery (e.g., Bechtel et al., 2004), logistic regression modelling (e.g., Mladenoff et al., 1995, 1999), multiple-criteria or decision rule analysis (e.g., Store & Kangas, 2001), and use of genetic algorithms such as GARP (Genetic Algorithm for Rule Set Production; e.g., Stockwell & Peters, 1999). Habitat mapping and modelling studies often make use of remotely sensed data, and recently Gottschalk et al. (2005) carried out a comprehensive review of 109 representative studies over the past 30 years that dealt with avian habitat and remote sensing. They found that most avian habitat studies investigate relationships of land cover or vegetation structure derived from satellite imagery with species occurrence taken from bird survey data. More recently, Tuttle et al. (2006) used ASTER satellite imagery to distinguish differences in vegetation and structure between territories of two types of sparrows in the Adirondack Mountains of New York. They found significant spatial and spectral differences in the imagery, although they did not attempt to use this information to map territories and/or habitat.

Previous habitat mapping efforts specifically for the hooded warbler have followed the aforementioned procedures. Pither (1997) found that patch area and soil properties were significantly related to hooded warbler presence however, the resultant models were quite poor, with predictive accuracy of approximately 36%. Mitchell et al. (2001) found overstory height and the number of understory vines to be significant predictors of hooded warbler presence in South Carolina, although the habitat characteristics of this southern state were quite different from those of this study in Canada. Flaxman (2004) performed habitat suitability modelling across southern Ontario using land cover type, patch size, land cover diversity (all derived from Landsat data), and terrain elevation surrounding nest sites. While the models were able to explain the presence of 64–72% of nest sites, suitable habitat was overestimated, causing up to 51% commission errors. It was concluded that better vegetation maps and higher resolution satellite imagery were needed in order to improve mapping of hooded warbler nesting habitat.

The current study addressed these recommendations through the use of Ikonos data and is one of the first studies to use high resolution satellite imagery to model avian habitat (see Gottschalk et al., 2005). The study also attempted to improve

Fig. 2. Multispectral Ikonos color infrared composite showing the training and validation sites used in local habitat mapping.

on previous mapping efforts by including image spatial and structural information linked to canopy gap characteristics associated with hooded warbler nesting habitat. To do this, and to provide more quantitative evidence of gap-nest associations than had been previously reported, an initial field study was conducted using hemispherical photography (Jennings et al., 1999; Pellikka et al., 2000). Previously, field studies had used ocular (sighting) tubes (B. Stutchbury, *pers. comm.*, 2005) to measure forest cover directly over nest sites. Hemispheric photography provides capability for estimation of cover at different zenith angles (Martens et al., 1993) and estimation of relative gap size and the gap size distribution within small angles from vertical. It also provides an archival image of the canopy, which is very useful for visual examination of the gaps (Chen et al., 1997).

The primary objectives of the research were:

1. Determine if reduced canopy cover and the presence of large gaps are quantitatively associated with hooded warbler nest locations.
2. Based on the results from Objective 1, determine if spectral and spatial image characteristics in high and moderate resolution remotely sensed data differ between nest and non-nest sites.
3. Evaluate the potential to exploit these image characteristics in mapping of potential hooded warbler nesting habitat.

Objective 1 was addressed using analysis of skyward hemispherical images. For Objectives 2 and 3, local scale habitat modelling and mapping using high resolution Ikonos and moderate resolution Landsat imagery were conducted for a focal forest where most of Canada's hooded warbler pairs are known to nest. Then, the potential for regional habitat mapping was evaluated using Landsat imagery.

2. Study area

While hooded warblers are found in clusters in the Carolinian Forests of southwestern Ontario (Fig. 1), the largest population exists in and around St. Williams Forestry Station along the north shore of Lake Erie. The area includes some of the largest remaining woodlots in southwestern Ontario, such as South Walsingham Forest and Backus Woods (Whittam & McCracken, 1999). In Fig. 1, it is represented by the small box indicating the Ikonos image coverage, while Fig. 2 shows these forests in greater detail. These forests currently contain some of the best examples of Carolinian species remaining in Canada, including large concentrations of tulip trees (*Liriodendron tulipifera*) and black gum (*Nyssa sylvatica*) (Allair et al., 2002). All three forests have undergone various degrees of management through selective cutting. St. Williams, having undergone the most logging of the three, is currently about 26% deciduous, 29% coniferous, and 45% mixed forest (Whittam et al., 2002). South Walsingham Forest was not used as extensively for logging and is therefore dominated by deciduous trees, with an approximate composition of 75% deciduous, 3% coniferous, and 22% mixed forest (Whittam et al., 2002). Backus Woods is mostly a mature deciduous forest with naturally created canopy gaps from infrequent disturbances (Allair et al., 2002).

The regional scale Landsat analysis was carried out across most of the full geographic extent of potential hooded warbler

nesting habitat in Canada, which included forests across southwestern Ontario from Toronto to Lake Huron and south to near Windsor (Fig. 1). A third Landsat scene would have been required in order to provide full coverage of the Ontario Carolinian forests, which extend west to Windsor, however no hooded warbler nests have been found in this area.

3. Methods

3.1. Field study of canopy gap characteristics associated with hooded warbler nesting habitat

Objective 1, to quantitatively determine if forest cover and gap size are associated with hooded warbler nest sites, was addressed through field data acquisition and analysis. This analysis is presented here to provide background context for the remote sensing research, including evaluation of links between gap and image characteristics. Field data were collected in July 2004 during the nesting season. Only Carolinian hardwood forests were sampled; the few untouched pine plantations in the area were excluded from the analysis because they generally had no ground vegetation except along access roads. With the aid of a Bird Studies Canada hooded warbler specialist, 24 known nest sites in the local forests (shown as 'training nest sites' in Fig. 2) were visited, providing a good distribution across the area. Nest sites had originally been located by researchers using the presence of a singing male in the area. Once their territory was established, the female and/or nest was searched out and flagged, as well as georeferenced with a GPS (Badzinski, 2003; Whittam & McCracken, 1999).

Areas unsuitable for nesting were more difficult to find as Bird Studies Canada uses the criterion that ground vegetation capable of supporting a nest must be absent and such locations were very rare. Many sites were visited that were initially thought to be unsuitable for nesting based on general site characteristics, however, even experienced hooded warbler researchers could not be completely certain (B. McLeod, *pers. comm.*, 2004). As a result, only one region of St. Williams forest was deemed to be absolutely unsuitable for nesting. It had very little ground vegetation and had been searched intensely without finding any nests in the past few years. Within this area, a random initial site was selected and twenty-one sample locations (Fig. 2) were marked out along a 300 m transect, staking every 10 m up to 100 m, and then every 20 m up to 300 m. The 10 m minimum spacing was deemed to provide spatial independence and was based on previous semivariogram range analyses of crown diameter in a hardwood forest near Ottawa (Butson & King, 1999). In addition, Jennings et al. (1999) pointed out that in measuring canopy cover, the spatial autocorrelation of crowns and canopy gaps must be taken into consideration, and sample sites must be separated by at least the size of the major spatial feature (the crowns, which were typically less than 10 m in diameter). This sample design provided 21 non-nesting sites.

The coordinates of each site were measured using a Trimble Geo XT Real-time differential GPS with WAAS corrections (FAA, 2005) that provided sub-meter accuracy (Trimble Navigation Ltd., 2004). Hemispherical digital camera images were acquired at each site for gap analysis using a Nikon Coolpix 990 digital camera with a Nikon Fisheye FC-E8 lens. Images were acquired under diffuse sky conditions to minimize direct scattering of sunlight off leaves and trunks (Olthof et al., 2003). The camera was mounted on a tripod with its major axis pointing north and levelled at a height of 1.5 m. A *k*-means unsupervised clustering algorithm was used to convert each image from raw 24-bit colour TIFF format into a binary canopy/gap image. Hemiview Canopy Analysis Software v2.1 (Delta-T Devices Ltd., 1999) was used to calculate the gap fraction (proportion of visible sky) in each image, which was then converted to percent cover. Overhead cover estimates were extracted for two zenith annuli of 0–15° and 15–30°, referred to hereafter by their centre angles 7.5° and 22.5°, respectively. These annuli are commonly used with hemispherical photography and other gap fraction sensors such as the Li-Cor LAI-2000 Plant Canopy Analyzer (Chen & Cihlar, 1996; Li-Cor Inc., 1991; Seed & King, 2003).

Percent cover estimates at nest and non-nest sites were compared using the Mann–Whitney *U* test (Bisson & Stutchbury, 2000), which was selected instead of a parametric *t*-test for consistency throughout the research since many variables tested were non-parametric. The size of overhead (7.5° zenith) gaps, the number of gaps, and the average and maximum gap size at each site (7.5° and 22.5° zenith) were calculated and compared between nest and non-nest sites. Relative gap areas were determined using the number of pixels in each gap. Absolute gap size (in m^2) was only estimated for the 7.5° zenith annulus, as larger angles include significant geometric distortions. For an approximate tree height of 23 m (Bisson & Stutchbury, 2000), and taking into account a tripod height of 1.5 m, the field-of-view at the top of the canopy for this angle (0–15°) was estimated to be 11.52 m in diameter, or 104.23 m^2. With 45,763 pixels in this field of view, each pixel represented 0.00228 m^2. This value was used to approximate the average, standard deviation, and maximum gap sizes for comparison between nest and non-nest sites.

3.2. Satellite imagery and initial processing

Ikonos-2 multispectral and panchromatic data were acquired July 3, 2004 for a 15 km × 13 km area covering the local study area (Fig. 2). The imagery was georeferenced using 17 ground control points, for which GPS positions had been collected, and a first order nearest neighbour transformation, resulting in an RMS error of 0.58 m (*x*) and 0.82 m (*y*). All non-forest was masked out from the imagery using an unsupervised *k*-means clustering.

Two Landsat-5 scenes were acquired for southwestern Ontario on June 4th 2004 (Path 18 Row 30) and September 15th 2004 (Path 19 Row 30), both of which were during full leaf-on conditions. Their combined coverage is shown in Fig. 1. The large difference in acquisition date was not ideal, but these were the only cloud-free images available from the growing season of 2004. It was deemed better to use imagery from the same year as the field data acquisition than to use previous

years' imagery, which also was not completely cloud-free, and may have introduced error caused by forest gap dynamics from year to year. Relative calibration was performed to minimize reflectance differences in forested areas between the two scenes. A simple Manual No-Change Regression (MNCR) approach was used (Over et al., 2003), which compares a set of dark and bright unchanged areas in both images. The quality of the calibration procedure was tested by comparing average and standard deviation brightness values between forests for each scene. The green, red, NIR, and MIR2 (Band 7) bands were highly correlated between scenes in the overlapping area, and therefore retained for further analysis with differences in average forest DN values having been reduced from as much as 30%, to less than 10%, while the blue and MIR1 (Band 5) bands were dropped due to poor correlation between scenes. The potential information content related to nesting habitat canopy characteristics that was lost by excluding these bands was probably small in comparison to the scene to scene differences that would have been included by retaining them because the MIR2 band was highly correlated with the MIR1 band ($r=0.95$) and the blue band was highly correlated with the green band ($r=0.97$). Following calibration, a mosaic was produced using a first order nearest neighbour transformation, with an RMSE of 0.61 m (x) and 0.51 m (y). The mosaic was then georeferenced, with an RMSE of 0.61 m (x) and 0.62 m (y), using a nearest neighbour second order transformation and 38 GCPs collected at road intersections throughout the imagery. All non-forest was masked out for further analysis using an unsupervised k-means clustering.

3.3. Database of nest and non-nest sites used for local and regional mapping

The 24 nest sites found in the summer of 2004 were combined with a database of nest sites found between 2002 to 2004 across southwestern Ontario ($n_{tot}=279$). This database was compiled from a variety of sources, including the Hooded Warbler/Acadian Flycatcher database (maintained by Bird Studies Canada), University of Toronto (S. Melles, Ph.D. candidate), and the 2nd Ontario Breeding Bird Atlas (2001–2005). Only locations with GPS coordinates were retained (all of these site locations were non-differentially corrected). Additionally, most of the nest sites had been given a score based on the quality of evidence of breeding: 1. Species observed in breeding season (no evidence of breeding), 2. Possible breeding, 3. Probable breeding, and 4. Confirmed breeding (OBBA, 2003). For the purpose of this research only the two highest levels (3 and 4) were used (K. Lindsay, *pers. comm.,* 2004) to provide strong evidence of breeding habitat. Table 1 summarizes the database sample numbers used at each scale in training and validation.

For local area nesting habitat modelling and mapping using Ikonos data, the 24 nest sites found in 2004 for the hemispherical photography analysis and the 21 non-nest sites along the transect in St. Williams Forest were used as training data because they represented the best evidence of nesting and non-nesting habitat closest in time to the image acquisition. From the Ontario database described above, 157 nest sites that were within the Ikonos coverage were set aside to use for model validation. Non-nest validation sites did not exist in the local area; it was not deemed appropriate to use some of the 21 non-nest sites on the St. Williams Forest transect for validation due to their spatial proximity to the remaining sites that would have been used for training. For Landsat modelling and mapping in the local area the same nest and non-nest sites as described above were used, but for nest site validation, eight sites were removed that were in very small forest patches that were not classified as forest in the Landsat classification (leaving 149 validation nest sites).

Table 1
Numbers of nest sites and sites not suitable for nesting used in training and validation for the local and regional scale analyses

	Nests		Non-nests	
	Training	Validation	Training	Validation
Local (Ikonos)	24	157	21	–
Local (Landsat)	24	149	21	–
Regional (Landsat)	140	139	38	25

For regional scale habitat modelling and mapping, all 279 nest sites from the entire Landsat coverage were randomly allocated to two groups for training and validation ($n=140$ and 139, respectively). In addition to the 21 non-nest sites on the St. Williams Forest transect, 42 additional sites not suitable for nesting (with no ground vegetation) were located across the region. These sites were selected in accessible forest patches large enough to be distinctly visible in the Landsat imagery. While there was a possibility that nests existed in these areas (a common problem in non-habitat selection for modelling (Kery & Gregg, 2003)), each area was searched intensively and they all had no ground vegetation suitable for nesting. The combined set of 63 non-nest sites was randomly split in a 60:40 ratio for training and validation.

3.4. Extraction of image information

The hemispherical photography analysis revealed greater canopy heterogeneity at nest sites (as described in detail in Results and discussion), which was expected to translate into greater brightness variations in the imagery. The shadows that exist in forest canopies as a result of the geometry and spacing of individual tree crowns cause a reduction in mean canopy reflectance and an increase in the spatial variation of reflectance (Seed & King, 2003), with the exception of very large gaps that result in direct illumination of the forest floor or understory. Based on these results, image texture measures and sub-pixel spectral unmixing, which can provide information on the fractions of the pixel that are shadow, sunlit crown or soil/background (Lévesque & King, 2003), were investigated in addition to image spectral variables for modelling and mapping potential nesting habitat.

Using a 5 × 5 (20 m × 20 m) window for the Ikonos imagery and a 3 × 3 (75 m × 75 m) window for the Landsat imagery, mean spectral brightness in each band and a selection of six commonly used co-occurrence matrix (GLCM) texture measures (Haralick

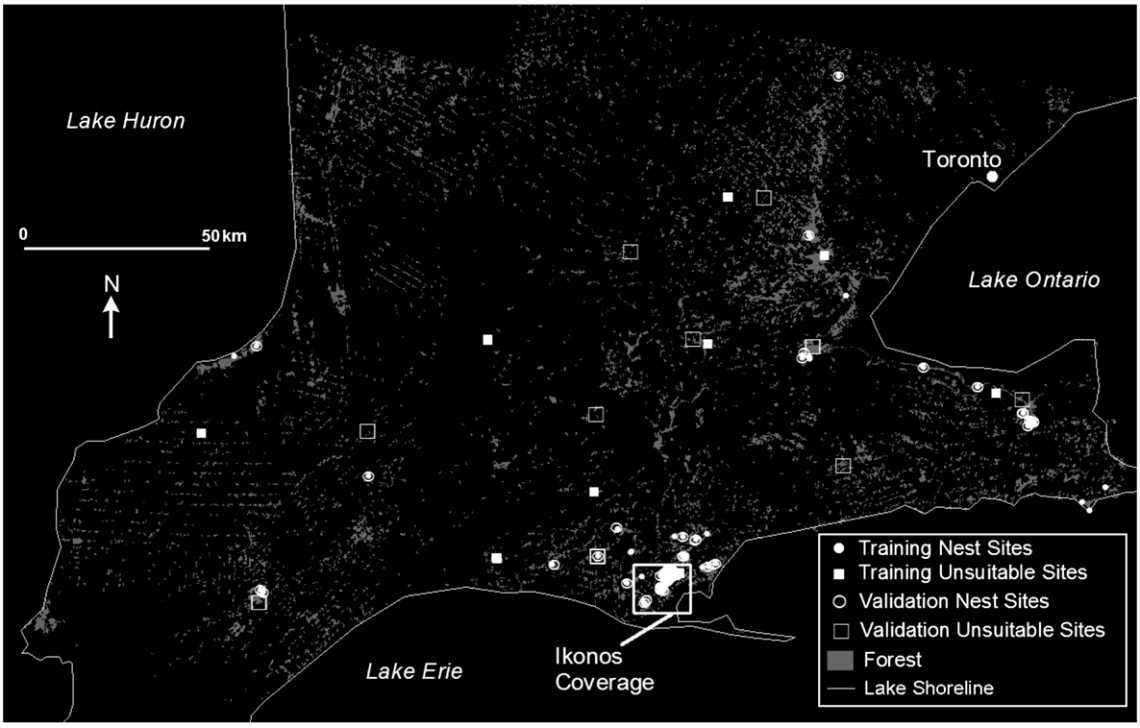

Fig. 3. Distribution of forests in southwestern Ontario and the training and validation sites used in regional habitat mapping. (Black background is masked out non-forest areas).

et al., 1973) were extracted for each site (Homogeneity, Contrast, Dissimilarity, Entropy, Angular Second Moment, and Correlation). Various studies have found certain GLCM textures to be useful for classification and vegetation structure modelling (e.g. Chan et al. (2003), Coburn and Roberts (2004) using Landsat; Tso and Olsen (2004) using Ikonos; Cosmopoulos and King (2004) using 0.5 m resolution airborne imagery). In particular, Tuttle et al. (2006) found significant differences between two types of sparrow habitat using image textures derived from ASTER imagery with 15 m pixels.

For the Ikonos analysis, the 5×5 window size was selected as it corresponded to the approximate view area (24.8 m diameter) in the canopy that was covered by the 30° outer zenith angle of the second annulus in the hemispherical photographs. A 3×3 window was also tested but classification results improved in all cases when the 5×5 window was used. The window size for Landsat analysis was the smallest possible to avoid deriving texture from pixels far from nest locations. Single pixel values for spectral brightness were extracted from the Landsat imagery and tested in classification, but accuracy did not improve.

Sub-pixel fractions of sunlit canopy, soil, and shadow were calculated from the imagery using a constrained least squares linear spectral unmixing algorithm (PCI Geomatics, 2004). Fraction averages in 5×5 and 3×3 windows were extracted from the Ikonos and Landsat imagery, respectively. Three different end member (EM) selection methods were tested: 1. manual delineation of pure areas of each EM within the imagery; 2. selection of pure areas directly from graphical representations of the *n*-dimensional spectral space (Van der Meer & de Jong, 2000); 3. automatic EM selection based on an iterative error analysis algorithm (Staenz et al., 1998). Results from each were very similar, so the manual delineation method was used for simplicity. Pure pixels did not exist for the shadow EM in the imagery, so deep water pixels, which had little to no reflectance in any spectral band, were used (Braun & Herold, 2003; Holben & Shimabukuro, 1993; Twele & Barbosa, 2004).

3.5. Comparison of image data at nest and non-nest sites

The second objective of this paper, to determine if canopy characteristics at nest and non-nest sites were associated with spectral and spatial image characteristics, was addressed by comparing the image variables using Mann-Whitney *U* tests between the nest and non-nest samples in both the Ikonos and Landsat imagery. Variables that did not show significant differences were dropped from further analysis. Those that were found to be significantly different ($p \leq 0.05$) were entered into a Principal Components Analysis (PCA) in order to create a reduced set of orthogonal variables, which explained a large proportion of the variance. These components were used as input variables for maximum likelihood classification and logistic regression modelling.

3.6. Maximum likelihood supervised classification

Supervised maximum likelihood classification was used to map potential nesting and non-nesting habitat in order to address the third objective of this research. For the local area

analysis, training and validation data locations are shown in Fig. 2 and the numbers of sites are given in Table 1. Training data were extracted from 5×5 pixel windows for the Ikonos data and 3×3 windows for the Landsat data, providing the mean and variance/co-variance matrices to be used for classification. Using these windows reduced the possibility of positional and radiometric errors associated with single pixel sampling, particularly for the high resolution Ikonos data. For regional classification with Landsat, the training and validation data locations are shown in Fig. 3 and the numbers of sites are given in Table 1.

All output classification maps were mode filtered using window sizes corresponding to those used for training in order to eliminate any single noise pixels. Tests showed that mode filtering eliminated single isolated pixels classified as either habitat or non-habitat while maintaining mapping accuracy. Also, for Ikonos mapping, the *a posteriori* class probabilities for nesting habitat were saved and analyzed further (e.g. as in Bastin, 1997).

To validate maps produced from Ikonos data for the local area, the 157 nest sites set aside were compared against their corresponding classified pixels. These validation nest sites may have contributed a small amount of error as the canopy may have changed and/or closed over during the one or two years since they had been found. Quantitative error analysis of unsuitable nesting habitat was not possible due to the lack of non-nest validation samples (all non-nest samples from the transect shown in Fig. 2 were used in training). Instead, visual assessment of the patterns of classification was conducted in relation to the known pattern of recent nests and areas not recently used for nesting. Similar methods were used for the local area Landsat analysis. In addition, the Landsat classification was cross tabulated with the Ikonos classification to determine the spatial coincidence of nesting habitat in both maps. Significant agreement between them, coupled with high nest habitat accuracy in the Ikonos map, would provide justification for continuing with regional mapping using the Landsat data.

Validation of regional scale Landsat maps was conducted using error matrices constructed from the 139 nest and 25 non-nest validation samples that were not used in training (Table 1).

3.7. Binary logistic regression

Used by many researchers for modelling habitat (e.g., Manel et al., 1999; Mladenoff et al., 1995, 1999; O2 Planning and Design, 2003), binary logistic regression was used to map potential hooded warbler nesting habitat. Local scale analysis was conducted using the Ikonos data and regional scale analysis was conducted using the Landsat data. The reduced set of image principal components, created as described previously, were used as independent variables with nest sites (presence) and non-nesting areas (absence) as the dependent variable. Binary logistic regressions were run with a 95% significance level. Forward stepwise regression was used for initial exploration, however, following this, Akaike's information criterion for small samples (AIC_c) (Sugiura, 1978) was applied in order to verify that the best model was indeed selected. Models were evaluated based on the Nagelkerke r^2 goodness-of-fit (Nagelkerke, 1991; SPSS, 2004), as well as using Receiver Operating Characteristic (ROC) curves calculated using the saved predicted probabilities of the models. The asymptotic significance of the ROC curves was examined along with the area under the curves, which ranges from 0 to 1, with a value of 0.5 indicating that the model was no better than a random guess, and a value of 1 representing "perfect discrimination" (Elith et al., 2006; Pearce & Ferrier, 2000).

4. Results and discussion

4.1. Canopy gap characteristics using hemispherical photography

As expected, percent cover was greater for both nest and non-nest sites in the 22.5° zenith angle than in the 7.5° view angle because it was more oblique and included more crown volume. Total canopy cover at nest sites was significantly lower than at non-nest sites for both zenith angles ($p=0.035$ at 7.5°, and $p=0.010$ at 22.5°). This was primarily due to large differences in the north to northeast azimuth direction.

Average gap size (in pixels) was significantly greater at nest sites in the 22.5° zenith angle ($p=0.017$). For the 7.5° zenith, variability was so great that no significant differences were found. For this view angle, average gap size was 5.09 m^2 (range=0–104.26 m^2) at nests and 0.25 m^2 (range=0.04–0.65 m^2) at non-nest sites. These results are greatly influenced by the extremely large number of tiny gaps in the canopy and as a result, the numbers of gaps at nest and non-nest sites were also not significantly different. Maximum gap size (in pixels) was significantly larger at nest sites for both the 7.5° and 22.5° zenith angles ($p=0.053$ and $p=0.008$, respectively). On average, the largest gap above nest sites was comprised of three to four-times the number of pixels as the largest gap at non-nest sites. For the 7.5° zenith angle this corresponded to average maximum gap sizes of 27.26 m^2 for nests versus 9.33 m^2 for non-nests, although, again, the ranges were large. These significant differences are useful as descriptors of overall canopy conditions, but they should not be used to characterise whether an individual site is potential nest habitat. In terms of potential impact on remotely sensed imagery, average maximum gap sizes of about 1.5 Ikonos pixels and average cover about 15% lower at nest sites were expected to increase image texture and perhaps the shadow fraction, while reducing average image brightness.

While hemispherical photographs have been used to quantify canopy structure and light conditions in other applications (e.g., Weiss (1991) for overwintering sites of monarch butterflies (*Danaus plexippus*); Pringle et al. (2003) for thermal microenvironments of the Broad-headed snake (*Hoplocephalus bungaroides*)), prior to this study it appears that they had not yet been used for quantifying canopy cover and canopy gaps in relation to bird habitat. All previous studies investigating cover relations to hooded warbler nest site selection, including Whittam and McCracken (1999), Bisson and Stutchbury (2000), used sighting tube methods. This research provides

more quantitative evidence that hooded warblers tend to build their nests in the presence of overhead canopy gaps. Such gaps have been shown to affect the succession and success of various understory species, which take advantage of the increased light conditions (Rankin & Tramer, 2002).

4.2. Local mapping with Ikonos imagery

From the Ikonos imagery, significant differences were found between nest and non-nest sites for several image variables. As expected, texture was significantly greater ($p<0.05$) at nest sites, specifically for ten of the twelve green and red band textures (not Correlation texture in both cases) and one of the NIR textures (Homogeneity). This indicated that the spatial variability of image brightness was greater around nest sites than non-nest sites. Brightness in the blue, green, and red was significantly greater while the shadow fraction was lower at nest sites, all of which were contrary to expectations. The reasons are not well understood at this time and warrant further research. The soil fraction also showed a significant difference, but the fractions for both nest and non-nest sites were so small (0.01 and 0.00, respectively) that they may be a result of unmixing error. For the variables that showed significant differences, all p values were less than 0.024.

Principal components (PCs) were created from the fifteen image variables that showed significant differences between nest and non-nest sites. The first two PCs accounted for 95.9% of the variance (PC1=67.6%, PC2=28.3%). PC1 was positively correlated with the visible bands and negatively correlated with the shadow fraction, while PC2 showed strong negative correlations with green and red texture. These two PCs were used as input variables in supervised classification. PC3 was excluded as it only accounted for 2.17% of the data variance, all factor loadings were <0.18, which was felt to be within the noise range in the data, and it was not significantly correlated with any of the spectral or texture inputs. Training data for nest and non-nest sites had a Transformed Divergence separability (Jensen, 2005) of 1.64, which was considered moderate.

Maximum likelihood classification produced a map composed of 92.2% potential nesting habitat and 7.8% unsuitable nesting habitat. Of the 157 validation nest sites, 109 (70%) were in pixels classified as nesting habitat. When an area of St. Williams Forest was examined in more detail (Fig. 4) it was found that many of the incorrectly classified nest sites were located very close to a nest/non-nest boundary. Distance to classified nest habitat was therefore measured and it was found that 28 of the 48 incorrect validation nest sites were within 10 m of nesting habitat. This error, to be conservative, could easily be attributed to a combination of the GPS measurements taken at these sites, which had not been differentially corrected (D. Badzinski, *pers. comm.*, 2004), and image geo-referencing error. Thus, a total of 87.3% of validation nest sites was in or within 10 m of classified nesting habitat. The distribution of *a posteriori* probabilities from the maximum likelihood classification algorithm (Table 2) showed 62.5% of the validation nest sites being in pixels classified as habitat with high probability (>0.70 (O2 Planning and Design, 2003)). In visual assessment of the classification of non-nesting habitat in St. Williams Forest, several large areas where nests had not been found in the past few years (Ellipses in Fig. 5) were well classified as non-nesting habitat, including the transect used for training.

Stepwise logistic regression using the two PCs produced a model with PC1 as a predictor of nest presence. The model's Nagelkerke r^2 was 0.50, indicating that half of the variance in the dataset was accounted for, with the ROC curve showing that

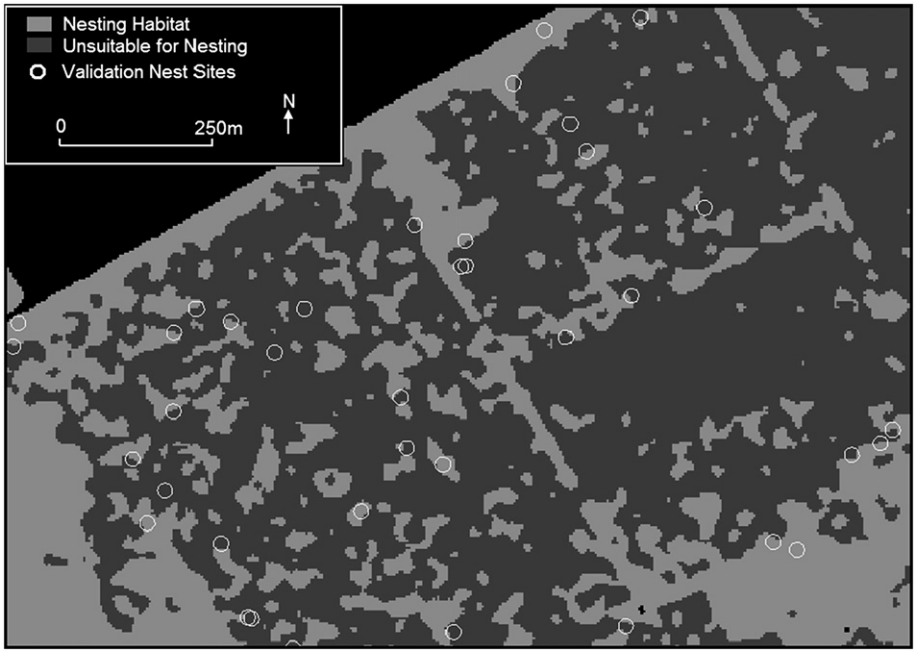

Fig. 4. A zoomed in portion of St. Williams Forest showing many validation nest sites located close to Ikonos classified nest habitat. Black background is masked out non-forest areas.

Table 2
Distribution of validation nest sites across Ikonos maximum likelihood (MLC) *a posteriori* probabilities and logistic regression probabilities

	% of validation nests	
Probability	MLC	Logistic regression
0.0–0.1	15.3	0.6
0.1–0.2	8.3	4.5
0.2–0.3	1.9	8.9
0.3–0.4	3.2	8.3
0.4–0.5	3.2	3.2
0.5–0.6	3.2	10.2
0.6–0.7	2.6	3.2
0.7–0.8	2.6	5.1
0.8–0.9	3.8	16.6
0.9–1.0	56.1	39.5

the model was a significant predictor of nest sites. The asymptotic significance was calculated to be 0.00, with values less than 0.05 indicating that the model was better than simply guessing with respect to classifying nest and non-nesting sites (SPSS, 2004). The area under the curve was found to be 0.87, indicating that if one nest site and one non-nesting site were selected at random from the dataset there would be a 0.87 probability that the predicted value for the nest site would be higher than the non-nesting site (Pearce & Ferrier, 2000). Additionally, it was found that the model correctly predicted 76% of the training nest sites. The distribution of the probabilities (Table 2) was similar to the maximum likelihood *a posteriori* probabilities, showing 61.2% of the validation nest sites with high probability ($p>0.70$). When the logistic regression probabilities were compared to the maximum likelihood probabilities, they showed quite good agreement with a Pearson correlation of 0.82 ($p<0.001$). However, the nests with low probabilities were spread throughout the range of 0–0.7, without a cluster near the low end that occurred for the maximum likelihood classifier.

The AIC_c analysis supported these results. As recommended by Sugiura (1978), since the sample size used was relatively small compared to the number of parameters, the corrected AIC was used. Three logistic regression models were run using the ENTER method (variables forced into the model), one using PC1, a second using PC2, and a third using PC1 and PC2, and the AIC_c was calculated for each model. The results showed clearly that the model with only PC1 as a predictor had the lowest value ($AIC_c=43.39$), confirming that it was the best (Anderson et al., 1994).

4.3. Local mapping with Landsat imagery

In Landsat mapping of the local area, the green, red, and MIR2 spectral band brightness and four textures (red Entropy and Angular Second Moment; MIR2 Entropy and Homogeneity) were significantly lower ($p<0.05$) for nest sites than for non-nest sites. Both the soil and shadow fractions showed significant differences, with soil significantly less, and shadow significantly greater at nest sites. PCA using these nine image

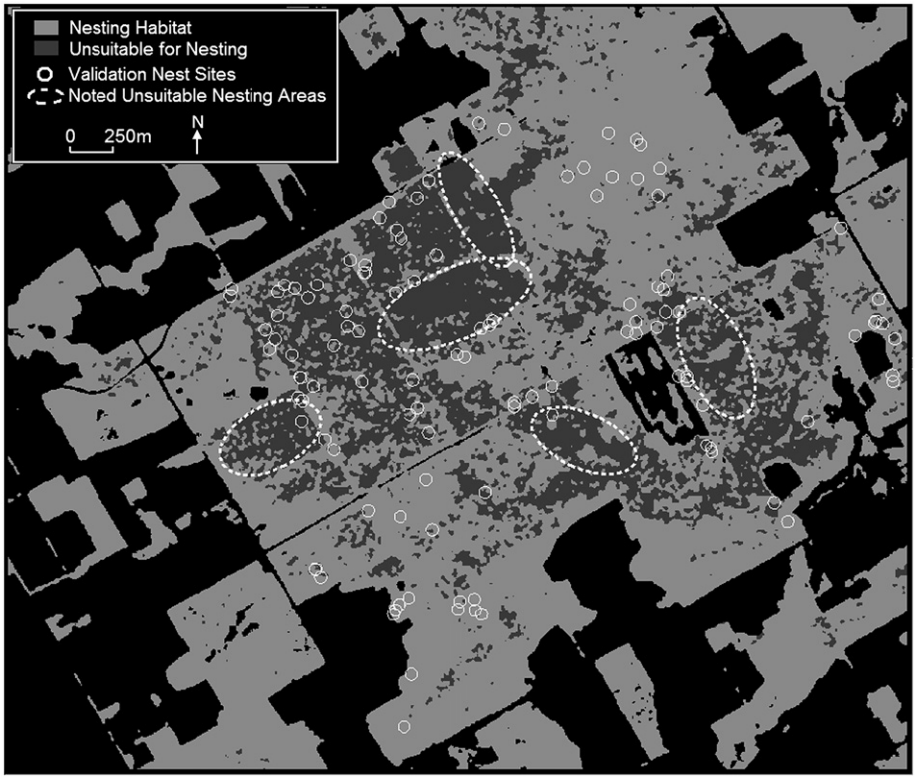

Fig. 5. Portion of the Ikonos classification centered on St. Williams Forest. Ellipses show areas classified as non-nesting habitat that have not recently been used for nesting (although most had some ground vegetation), including the non-nest transect area used for training. White circles are used to symbolize nest sites, which are located at the center of the circles. Black background is masked out non-forest areas.

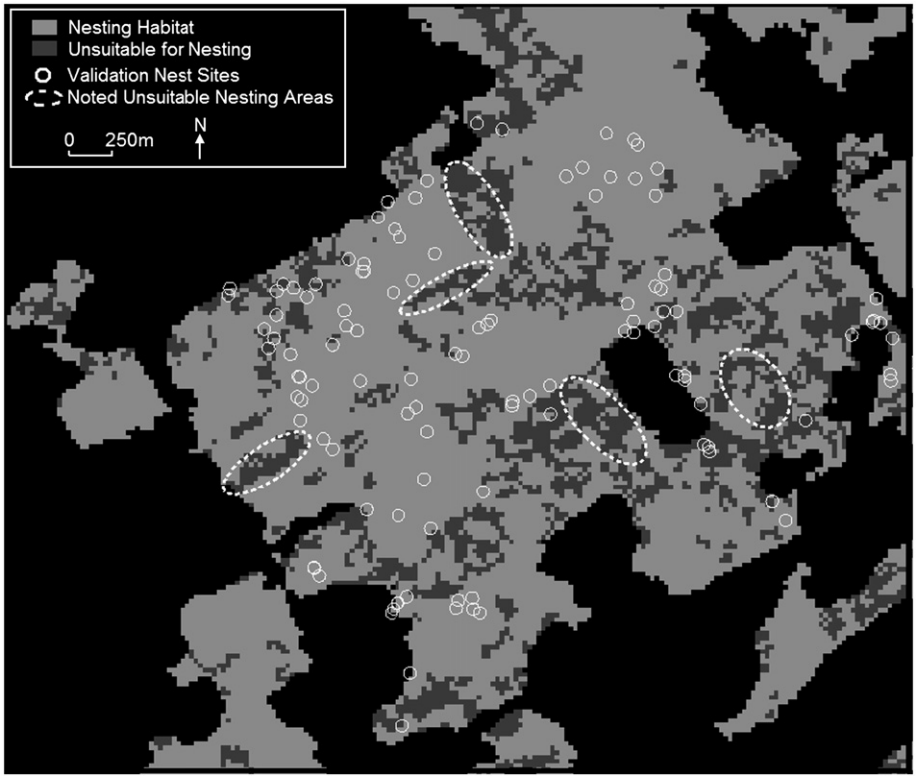

Fig. 6. Portion of the Landsat classification centered on St. Williams Forest that was created from local training data. Ellipses show areas classified mostly as non nesting habitat that have not recently been used for nesting, including the non-nest transect area used for training. Black background is masked out non-forest areas.

variables produced four PCs that accounted for 96.7% of the data variance (PC1=49.1%, PC2=39.2%, PC3=6.0%, and PC4=2.4%). Factor loadings showed that the first three PCs represented various red and mid-infrared textures. The fourth PC, although representing such a low percentage of the variance, had a high Pearson correlation with the shadow fraction (r=0.89) so it was retained. Maximum likelihood classification was conducted using the same training sites as in the Ikonos classification and these four PCs as input variables.

The output map for the area centered on St. Williams Forest is shown in Fig. 6. The areas surrounding St. Williams Forest appear visually different from the map created from the Ikonos imagery (Fig. 5) because of differences in the non-forest masks that had been individually delineated at the two image scales. The Landsat classification results showed that 87% of the validation nest sites were correctly classified, but much more of St. Williams Forest appeared to be classified as nesting habitat compared to the Ikonos map. As in classification using the Ikonos data, quantitative assessment of non-nesting accuracy was not possible with the Landsat map due to a lack of validation non-nesting sites in the area. However, similar to the Ikonos results, areas known to have been unoccupied by nest sites in recent years (ellipses in Fig. 6) were well classified as non-nesting habitat (although not as spatially complete as in the Ikonos map).

Resampling the Landsat map to the same pixel size as the Ikonos map and cross tabulating them showed that 80% of the habitat pixels in St. Williams Forest matched in both classifications. However, only about 30% of the non-habitat regions matched at the pixel level due to many small areas classified in the Ikonos imagery that were not detected in the Landsat imagery. Based on the above assessment, it was concluded that Landsat is suitable for local mapping of general hooded warbler habitat patterns but that more spatial detail related to smaller gaps and canopy heterogeneity can only be achieved with higher resolution imagery such as Ikonos. The next step was to determine if Landsat could be applied over the broader region of southwestern Ontario.

4.4. Regional mapping with Landsat imagery

Regional maximum likelihood mapping with Landsat using training and validation data collected from throughout southwestern Ontario did not produce results that were as good as the local area mapping. The training data Transformed Divergence was only 0.20, indicating almost complete overlap between the two classes. The classification error matrix for the validation data had an overall Kappa coefficient of 0.17, indicating that the classification was only 17% better than random (Foote & Huebner, 2000) (Table 3). The map was extremely grainy in many places and did not provide accurate representations of habitat and non-habitat in known areas such as St. Williams forest. It was almost completely classified as nesting habitat, including the known distinct non-nesting transect (Fig. 2) and the areas known to have not had nests in recent years (ellipses in Fig. 5). The net result was an overestimation of potential habitat, similar to Flaxman's (2004) research.

Table 3
Error matrix for regional mapping with Landsat: (a) training data, (b) validation data

		Field class	
		Nests	Non-habitat
Image class	(a)		
	Nesting habitat	101 (72%)	15
	Non-habitat	39	23 (60%)
	(b)		
	Nests	101 (73%)	12
	Non-habitat	38	13 (52%)

The results produced from logistic regression modelling using the Landsat data were also disappointing; no significant models were created. This may have been partially because most nest sites were within St. Williams Forest, in which most of the Canadian population of hooded warblers is clustered. This forest had a distinct structure and composition (J. McCraken, *pers. comm.*, 2004) due to years of logging and tree planting. This is evident in the dark and varied tones of the forest in Fig. 2 in comparison to the nearby forests. South Walsingham Forest is somewhat similar and did have a higher population in the past when logging was ongoing, however, many of the forest gaps created by logging have filled in and the population has declined. The same process may occur in St. Williams Forest in the next five to ten years as logging has recently terminated there (Allair et al., 2002; Whittam et al., 2002).

The high error may also have been due to the disproportionate number of nest sites compared to unsuitable nesting sites used for training. To test this, the logistic regression was re-run twice using equal numbers of training and test samples. In each, sixty-three nest sites were randomly selected from the database of 279 (Table 1) to match the available 63 non-nesting sites. With these input data, very weak models were produced with Nagelkerke r^2 values of 0.18 and 0.11, respectively. Accuracies of predicted nest and non-nest sites were 65.0% and 74.6% (1st model), and 61.9% and 58.7% (2nd model). Based on these results it was concluded that a useful model could not be produced from this dataset, even using equal and adequate numbers of nest and non-nest sites.

5. Conclusions

While the underlying goal of this research was to identify potential hooded warbler nesting habitat in southwestern Ontario, there are only a few large forests remaining in the region. Flaxman (2004) showed that 96% of evaluated hooded warbler occurrences were in forest patches greater than 100 ha. Given the poor regional mapping results achieved with Landsat, it would be more beneficial to target each of the large remaining forests in southwestern Ontario for detailed habitat mapping with high-resolution sensors such Ikonos, Quickbird, or airborne multispectral/hyperspectral sensors. These data types are best for targeting local sites because acquiring coverage of large areas is extremely costly and perhaps not feasible. At a local scale, this study showed that classification or logistic regression using image spectral and spatial information can predict potential nest areas with high accuracy and produce maps with habitat/non-habitat spatial patterns that match well with actual field distributions. As gap dynamics affect hooded warbler nesting activity, high resolution remote sensing should be useful in monitoring temporal changes in the canopy and the spatial distribution of potential habitat.

The results of this research could potentially be used in management planning to maintain gaps in selected forests for provision of suitable hooded warbler habitat, or to maintain existing habitat. From a management perspective, understanding how much cover can be removed and the means by which it should be removed in order to provide such habitat is potentially an important part of population recovery and maintenance. In future work, other complementary remote sensors, such as lidar or radar, should be evaluated to provide more detail with regards to vertical forest structure. As well, other environmental variables of importance to hooded warblers could potentially be combined with forest structure and canopy gap information to improve habitat mapping accuracy.

Acknowledgements

This research was funded by the National Wildlife Research Centre (NWRC) as well as a grant to D. King from the Natural Sciences and Engineering Research Council of Canada (NSERC). Field data collection was greatly aided by the assistance of Robby Bemrose. Thanks to Bird Studies Canada, particularly Debbie Badzinski, for providing data, helpful insights, and field support. Rosalind Ford (Bird Studies Canada), Stephanie Melles and Brad McLeod (University of Toronto) provided additional data and field support. Environment Canada and the Ontario Ministry of Natural Resources provided key funding for the intensive field studies that were carried out by a variety of field staff on behalf of the national Hooded Warbler/Acadian Flycatcher Recovery Team, with the cooperation of many landowners. Thanks also to the sponsors of the Ontario Breeding Bird Atlas (Bird Studies Canada, Canadian Wildlife Service, Ontario Nature, Ontario Field Ornithologists, and Ontario Ministry of Natural Resources) for supplying Atlas data, and to the thousands of volunteer participants who gathered data for the Atlas project.

References

Allair, J., Badzinski, D., Whittam, B., & McCracken, J. (2002). *Southern Ontario hooded warbler research: 2001 final report.* Internal Report Port Rowan, Ontario: Bird Studies Canada.

Anderson, D. R., Burnham, K. P., & White, G. C. (1994). AIC model selection in overdispersed capture–recapture data. *Ecology*, *75*, 1780−1793.

Badzinski, D. S. (2003). *Hooded warbler research in St. Williams Forest, Ontario: An investigation of nest productivity, nest concealment, territory size and species associations.* Internal Report Port Rowan, Ontario: Bird Studies Canada.

Bastin, L. (1997). Comparison of fuzzy c-means classification, linear mixture modelling and MLC probabilities as tools for unmixing coarse pixels. *International Journal of Remote Sensing*, *18*, 3629−3648.

Bechtel, R., Sanchez-Azofeifa, A., Rivard, B., Hamilton, G., Martin, J., & Dzus, E. (2004). Associations between woodland caribou telemetry data and Landsat TM spectral reflectance. *International Journal of Remote Sensing*, *25*, 4813−4827.

Bisson, I. A., & Stutchbury, B. J. M. (2000). Nesting success and nest-site selection by a neotropical migrant in a fragmented landscape. *Canadian Journal of Zoology*, *78*, 858−863.

Braun, M., & Herold, M. (2003). Mapping imperviousness using NDVI and linear spectral unmixing of ASTER data in the Cologne–Bonn region Germany. *Proceedings of SPIE 2003, Barcelona, Spain* (pp. 274−284).

Butson, C., & King, D. J. (1999). Semivariance analysis of forest structure and remote sensing data to determine an optimal sample plot size. *Proceedings 4th International Airborne Remote Sensing Conference and Exhibition (Env. Res. Inst. of Michigan) / 21st Canadian Symposium on Remote Sensing (Canadian Remote Sensing Society), Ottawa, Ontario, June 21–24*, *Vol. II.* (pp. 155−162).

Chan, J. C. W., Laporte, N., & Defries, R. S. (2003). Texture classification of logged forests in tropical Africa using machine-learning algorithms. *International Journal of Remote Sensing*, *24*, 1401−1407.

Chen, J. M., & Cihlar, J. (1996). Retrieving leaf area index of boreal conifer forest using Landsat TM images. *Remote Sensing of Environment*, *55*, 153−162.

Chen, J. M., Rich, P. M., Gower, S. T., Norman, J. M., & Plummer, S. (1997). Leaf area index of boreal forests: Theory, techniques and measurements. *Journal of Geophysical Research*, *102*, 29429−29443.

Coburn, C. A., & Roberts, A. C. (2004). A multiscale texture analysis procedure for improved forest stand classification. *International Journal of Remote Sensing*, *25*, 4287−4308.

Cosmopoulos, P., & King, D. J. (2004). Temporal analysis of forest structural condition at an acid mine site using multispectral digital camera imagery. *International Journal of Remote Sensing*, *25*, 2259−2275.

Delta-T Devices Ltd. (1999). *Hemiview canopy analysis software.* Cambridge, UK: Delta-T Devices Ltd.

Elith, J., Graham, C. H., Anderson, R. P., Dudý´k, M., Ferrier, S., Guisan, A., et al. (2006). Novel methods improve prediction of species' distributions from occurrence data. *Ecography*, *29*, 129−151.

Environment Canada (2003). Species at risk website. http://www.speciesatrisk.gc.ca

Federal Aviation Administration (FAA) (2005). Wide Area Augmentation System (WAAS). http://gps.faa.gov/Library/waas-f-text.htm

Flaxman, M. (2004). *Habitat identification and mapping for the Acadian flycatcher, hooded warbler and prothonotary warbler in southern Ontario.* IRF Project #31. Contract report for NWRC, CWS, EC. K1A-0H3.

Foote, K. E., & Huebner, D. J. (2000). Calculating Cohen's kappa. http://www.colorado.edu/geography/gcraft/notes/manerror/html/kappa.html

Gottschalk, T. K., Huettmann, F., & Ehlers, M. (2005). Thirty years of analysing and modelling avian habitat relationships using satellite imagery data: A review. *International Journal of Remote Sensing*, *26*, 2631−2656.

Haralick, R. M., Shanmugan, K., & Dinstein, I. (1973). Textural features for image classification. *IEEE Transactions on Systems, Man, and Cybernetics*, *SMC-3*, 610−621.

Holben, B. N., & Shimabukuro, Y. E. (1993). Linear mixing model applied to coarse spatial resolution data from multispectral satellite sensors. *International Journal of Remote Sensing*, *14*, 2231−2240.

James, F. C., & McCulloch, C. E. (2002). Predicting species presence and abundance. In J. M. Scott, P. J. Heglund, M. L. Morrison, J. B. Haufler, M. G. Raphael, W. A. Wall, & F. B. Samson (Eds.), *Predicting species occurrences: Issues of accuracy and scale* (pp. 461−465). Washington: Island Press.

Jennings, S. B., Brown, N. D., & Sheil, D. (1999). Assessing forest canopies and understory illumination: Canopy closure, canopy cover and other measures. *Forestry*, *72*, 59−73.

Jensen, J. R. (2005). *Introductory digital image processing: A remote sensing perspective* (3rd Ed.). Upper Saddle River, NJ: Pearson Prentice Hall 526 pp.

Kery, M., & Gregg, K. B. (2003). Effects of life-state on detectability in a demographic study of the terrestrial orchid *Cleistes bifaria*. *Journal of Ecology*, *91*, 265−273.

Lévesque, J., & King, D. J. (2003). Spatial analysis of radiometric fractions from high-resolution multispectral imagery for modelling individual tree crown and forest canopy structure and health. *Remote Sensing of Environment*, *84*, 589−602.

Li-Cor Inc. (1991). *LAI-2000 plant canopy analyzer operating manual.* Lincoln, NE, USA: Li-Cor Inc.

Manel, S., Dias, J. M., Buckton, S. T., & Omerod, S. J. (1999). Alternative methods for predicting species distribution: An illustration with Himalayan river birds. *Journal of Applied Ecology*, *36*, 734−747.

Martens, S. N., Ustin, S. L., & Rousseau, R. A. (1993). Estimation of tree canopy leaf area index by gap fraction analysis. *Forest Ecology and Management*, *61*, 91−108.

Mitchell, M. S., Lancia, R. A., & Gerwin, J. A. (2001). Using landscape-level data to predict the distribution of birds on a managed forest: Effects of scale. *Ecological Applications*, *11*, 1692−1708.

Mladenoff, D. J., Sickley, T. A., Haight, R. G., & Wydeven, A. P. (1995). A regional landscape analysis and prediction of favorable gray wolf habitat in the Northern Great Lakes region. *Conservation Biology*, *9*, 279−294.

Mladenoff, D. J., Sickley, T. A., & Wydeven, A. P. (1999). Predicting gray wolf landscape recolonisation: Logistic regression models vs. new field data. *Ecological Applications*, *9*, 37−44.

Nagelkerke, N. J. D. (1991). A note on a general definition of the coefficient of determination. *Biometrika*, *78*, 691−692.

O^2 Planning and Design (2003). *Whooping crane potential habitat mapping project.* Contract report for NWRC, CWS, EC. K1A-0H3 46 pp.

Olthof, I., King, D. J., & Lautenschlager, R. A. (2003). Overstory and understory leaf area index as indicators of forest response to ice storm damage. *Ecological Indicators*, *3*, 49−64.

Over, M., Schöttker, B., Braun, M., & Menz, G. (2003). Relative radiometric normalisation of multitemporal Landsat data — A comparison of different approaches. *Proceedings of IGARSS, July 2003, Toulouse, France* (pp. 3623−3625).

Pearce, J., & Ferrier, S. (2000). Evaluating the predictive performance of habitat models developed using logistic regression. *Ecological Modelling*, *133*, 225−245.

Pellikka, P. K. E., Seed, E. D., & King, D. J. (2000). Modelling deciduous forest ice storm damage using CIR aerial imagery and hemispheric photography. *Canadian Journal of Remote Sensing*, *26*, 394−405.

PCI Geomatics (2004). www.pcigeomatics.com

Pither, R. (1997). An investigation into the use of satellite data and geographical information systems for developing habitat models of rare bird species in southwestern Ontario. M.Sc. Thesis. Department of Geography, University of Western Ontario, London, Canada.

Pringle, R. M., Webb, J. K., & Shine, R. (2003). Canopy structure, microclimate, and habitat selection by a nocturnal snake, *Hoplocephalus bungaroides*. *Ecology*, *84*, 2668−2679.

Rankin, W. T., & Tramer, E. J. (2002). Understory succession and the gap regeneration cycle in a *Tsuga Canadensis* forest. *Canadian Journal of Forest Research*, *32*, 16−23.

SARA (2005). Species at risk act public registry. http://www.sararegistry.gc.ca

Seed, E. D., & King, D. J. (2003). Shadow brightness and shadow fraction relations with effective leaf area index: Importance of canopy closure and view angle in mixedwood boreal forest. *Canadian Journal of Remote Sensing*, *29*, 324−335.

SPSS (2004). SPSS Inc. www.spss.com

Staenz, K., Szeredi, T., & Schwarz, J. (1998). ISDAS — A system for processing/analysing hyperspectral data. *Canadian Journal of Remote Sensing*, *24*, 99−113.

Stockwell, D. R. B., & Peters, D. P. (1999). The GARP modelling system: Problems and solutions to automated spatial prediction. *International Journal of Geographical Information Systems*, *13*, 143−158.

Store, R., & Kangas, J. (2001). Integrating spatial multi-criteria evaluation and expert knowledge for GIS-based habitat suitability modelling. *Landscape and Urban Planning*, *55*, 79−93.

Sugiura, N. (1978). Further analysis of the data by Akaike's information criterion and the finite correction. *Communications in Statistics. Theory and Methods*, *7*, 13−26.

Trimble Navigation Ltd. (2004). http://www.trimble.com

Tso, B., & Olsen, R. C. (2004). Scene classification using combined spectral, textual, and contextual information. In S. S. Shen & P. E. Lewis (Eds.), *Algorithms and Technologies for Multispectral, Hyperspectral, and Ultraspectral Imagery X, Proceedings of the SPIE*, *Vol. 5425*.

Tuttle, E. M., Jensen, R. R., Formica, V. A., & Gonser, R. A. (2006). Using remote sensing image texture to study habitat use patterns: A case study

using the polymorphic white-throated sparrow (*Zonotrichia albicollis*). *Global Ecology and Biogeography*, *15*, 349−357.

Twele, A., & Barbosa, P. (2004). Monitoring vegetation regeneration after forest fires using satellite imagery. *Proceedings of the 24th Symposium of the European Association of Remote Sensing Laboratories, Dubrovnik, Croatia, May 25–27, 2004* 9 pp.

Van der Meer, F., & de Jong, S. M. (2000). Improving the results of spectral unmixing of Landsat Thematic Mapper imagery by enhancing the orthogonality of EMs. *International Journal of Remote Sensing*, *21*, 2781−2797.

Weiss, S. B. (1991). Forest canopy structure at overwintering monarch butterfly sites: Measurements with hemispherical photography. *Conservation Biology*, *5*, 165−175.

Whittam, B., & McCracken, J. (1999). Productivity and habitat selection of hooded warblers in southern Ontario. *Internal Report* Port Rowan, Ontario: Bird Studies Canada 47 pp.

Whittam, R. M, McCracken, J. D., Francis, C. M., & Gartshore, M. E. (2002). The effects of selective logging on nest-site selection and productivity of hooded warblers (*Wilsonia citrina*) in Canada. *Canadian Journal of Zoology*, *80*, 644−654.